

# Numerical investigation of the curvature effects on diffusion flames

Peiyong Wang, Shengteng Hu, Robert W. Pitz \*

*Mechanical Engineering Department, Vanderbilt University, Nashville, TN 37235, USA*

## Abstract

Tubular diffusion flames are compared with opposed jet diffusion flames numerically to show the effect of curvature on diffusion flames. The numerical results show that, as in premixed flames, positive curvature strengthens the preferential diffusion and negative curvature weakens the preferential diffusion; the strengthening or weakening effect is proportional to the ratio of flame thickness to flame radius. Since the flame temperature is related to the preferential diffusion, flame curvature affects flame temperature and extinction stretch rate. As the flame thickness is related to pressure, the curvature effects also depend on pressure.  $H_2/N_2$ -air and  $CH_4/N_2$ -air diffusion flames with different flame radii and pressures are presented to verify the analysis.

© 2006 The Combustion Institute. Published by Elsevier Inc. All rights reserved.

*Keywords:* Stretch; Curvature; Opposed jet flame; Opposed tubular flame; Diffusion flame

## 1. Introduction

Stretched planar laminar diffusion flames realized by the opposed jet burner shown in Fig. 1 have been studied broadly and numerical solutions using commercial software (e.g., OPPDIF of CHEMKIN [1]) are available. Liñan [2] first studied this kind of diffusion flame and obtained analytical expressions for ignition and extinction. Chung and Law [3,4], and Cuenot and Poinso [5] analyzed the opposed jet diffusion flames with infinitely fast chemistry and non-unity Lewis numbers. It is shown that the preferential diffusion effect exists on both the fuel side and the oxidizer side of the flame. For example, when the Lewis number of the fuel or oxygen is less than

one, the flame temperature is higher than its adiabatic equilibrium temperature (with unity Lewis numbers, i.e.,  $Le_f = Le_o = 1$ , the flame temperature is a constant under the infinitely fast chemistry assumption [6] and is called the adiabatic equilibrium temperature); when the Lewis number of the fuel or oxygen is more than one, the flame temperature is less than its adiabatic equilibrium temperature; but the preferential diffusion effect is constant under infinitely fast chemistry, that is, the temperature increase or decrease is independent of stretch rate. With one-step high-activation-energy finite rate chemistry, Chung and Law [7], and Cuenot and Poinso [5] gave the flame temperature and extinction variation with stretch rate and Lewis numbers. Sung et al. [8] studied the opposed jet diffusion flame structure with complex chemistry and showed the influence of the chemical kinetics on the structure of the opposed jet flames. Brown et al. [9] studied the flame structure and preferential diffusion for

\* Corresponding author. Fax: +1 615 343 6687.

E-mail address: [robert.w.pitz@vanderbilt.edu](mailto:robert.w.pitz@vanderbilt.edu) (R.W. Pitz).

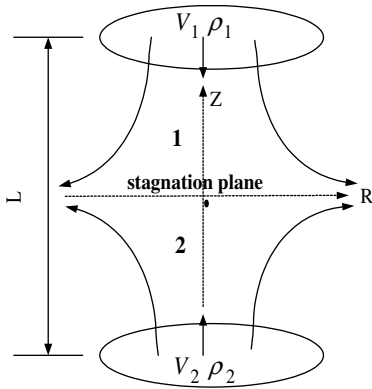


Fig. 1. Opposed jet burner schematic.

the opposed jet hydrogen flames experimentally. Both papers [8,9] show that the flame thickness is inversely proportional to the square root of stretch rate.

The study of the curvature effects on diffusion flames basically focuses on two flames: the flame tip of Burke–Schumann flames [10–15] and the perturbed opposed jet flames [16–21]. Ishizuka and co-worker [10,11] studied the extinction at the curved flame tip of Burke–Schumann flame experimentally; the local extinction at the tip was observed with the mixture of H<sub>2</sub> and CO<sub>2</sub> as the fuel stream. Im et al. [12] also studied the flame tip theoretically and experimentally; the flame tip is negatively stretched which increases the residential time of reactants in the reaction zone; it makes the flame tip stronger and harder to be extinguished. For a fuel stream with Lewis number less than one, the preferential diffusion results in low fuel concentration, low temperature and possible extinction at the flame tip. Katta et al. [13] and Takagi et al. [14,15] also studied similar flames numerically. In [15], the flame tip temperature is much lower than the adiabatic equilibrium temperature if the fuel (H<sub>2</sub>/N<sub>2</sub>, Lewis number less than one) comes from the inner nozzle, i.e. the flame is concave to the fuel stream and vice versa if the fuel comes from the outer nozzle; detailed numerical analysis on flame structure substantiated the preferential diffusion effect. Takagi et al. [16], Finke and Grünefeld [17], and Lee et al. [19] perturbed the opposed jet flame to form curved flames with positive stretch; the results are consistent with those from Burke–Schumann flames. When the flame is concave to the fuel stream (H<sub>2</sub>/N<sub>2</sub>), the flame is weaker and the local extinction is observed; the flame is stronger if the flame is convex to the fuel stream. In [18], for the same stretch rate, the flame has higher temperature if the flame is convex to the H<sub>2</sub>/N<sub>2</sub> fuel stream and lower temperature if the flame is concave to the fuel stream; the temperature difference increases as the stretch rate decreases.

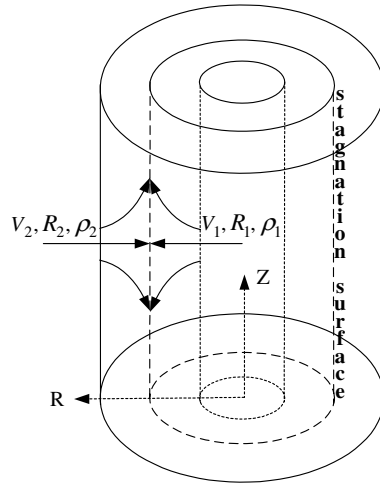


Fig. 2. Opposed tubular burner schematic.

For the Burke–Schumann flames and perturbed opposed jet flames, the flames are multidimensional and it is hard to identify the values of stretch rate and curvature; and sometimes, it is hard to separate the effects of stretch and curvature since the stretch rate and curvature vary simultaneously when the operational conditions are varied. To overcome these difficulties, the opposed tubular burner as shown in Fig. 2 was built and has been tested in [22]. The main advantages of this burner are: (1) the flame structure is one-dimensional; (2) the flame is uniformly stretched and curved; (3) stretch rate and curvature can be varied independently. Here, we compare the opposed tubular flame with the opposed jet flame numerically to study the curvature effects on diffusion flames.

## 2. Governing equations

A one-dimensional similarity solution is sought for the steady opposed tubular flame [23]. A stream function  $\psi(Z, R) = Zf(R)$  is assumed which satisfies the mass conservation exactly:

$$-\partial\psi/\partial R = R\rho U_Z = -Zdf/dR \text{ and}$$

$$\partial\psi/\partial Z = R\rho U_R = f, \quad (1)$$

$$g = -(df/dR)/(\rho R), \quad (2)$$

$$dJ/dR = 0, \quad (3)$$

$$f \frac{dg}{dR} = \frac{d}{dR} \left( \mu R \frac{dg}{dR} \right) - R(J + \rho g^2). \quad (4)$$

$U_R$  is the radial velocity that is a function only of  $R$  and  $U_Z$  is the axial velocity that is a linear function of  $Z$ . The temperature, species concentration,

density and transport coefficients are functions of  $R$  alone.  $J$  is the pressure eigenvalue  $J = (1/Z)\partial p/\partial Z$  that is a constant for certain boundary conditions [23–25].

The energy and species conservation equations are:

$$\rho C_p U_R \frac{dT}{dR} + \frac{1}{R} \frac{d}{dR} \left( -R\lambda \frac{dT}{dR} \right) + \rho \frac{dT}{dR} \left( \sum_i C_{pi} Y_i V_i' \right) + \sum_i h_i \varpi_i = 0, \quad (5)$$

$$\rho U_R \frac{dY_i}{dR} + \frac{1}{R} \frac{d}{dR} (R\rho Y_i V_i') - \varpi_i = 0, \quad (6)$$

$$V_i' = \frac{1}{X_i W} \sum_{j \neq i} W_j D_{ij} \frac{dX_j}{dR} - \frac{D_i^T}{\rho Y_i T} \frac{dT}{dR}. \quad (7)$$

The boundary conditions are:

$$R = R_1, \quad f = R_1 \rho_1 V_1, \quad g = 0, \quad T = T_1,$$

$$Y_i = Y_{i1},$$

$$R = R_2, \quad f = R_2 \rho_2 V_2, \quad g = 0, \quad T = T_2,$$

$$Y_i = Y_{i2}.$$

$T$  is the temperature;  $Y_i$  is the mass fraction of species  $i$ ;  $\lambda$  is the thermal conductivity;  $C_p$  and  $C_{pi}$  are the averaged specific heat and specific heat of species  $i$ , respectively;  $V_i'$  is the diffusion velocity of species  $i$ ;  $h_i$  is the enthalpy per unit mass of species  $i$  and  $\varpi_i$  is the mass reaction rate per unit volume of species  $i$ .  $X_i$  is the molar fraction of species  $i$ ;  $W_j$  and  $W$  are the molecular mass of the  $j$ th species and the averaged molecular mass;  $D_{ij}$  and  $D_i^T$  are the multi-component and thermal diffusion coefficients, respectively. A modified OPPDIF program is used to simulate the opposed tubular flame [23,26] with perfect gas law, complex chemistry and detailed transport properties. The OPPDIF program of CHEMKIN [1] gives the numerical solution for the opposed jet flame (one-dimensional similarity solution) and the conservation equations can be found in [27].

The boundary condition specifies the mass fraction and temperature. Extra mass diffusion from the nozzles and extra heat conduction to the nozzles exist if the species and temperature gradients are not zero at the nozzle exits. The enthalpy gain from the extra mass diffusion and the heat loss from the extra conduction generally are not balanced; this makes the flame temperature change and this change is not the result of stretch or curvature. In the following calculation, we did not include any results with either temperature or species gradients at the nozzle exits.

The numerical solution has been validated by the experimental data in Hu et al. [28]; the mea-

sured and predicted flame temperature, flame position and flame structure have very good agreement.

### 3. Stretch rates of the flames

Seshadri and Williams [29], Wang et al. [23] gave the expressions of stretch rate for the opposed jet burner and the opposed tubular burner respectively.

For the opposed jet flame [29],

$$\text{At side 1, } k = 2[|V_2|(\rho_2/\rho_1)^{0.5} + |V_1|]/L; \quad (8)$$

$$\text{At side 2, } k = 2[|V_1|(\rho_1/\rho_2)^{0.5} + |V_2|]/L. \quad (9)$$

For the opposed tubular flame [23]:

$$\text{At side 2, } k = -V_2 Q^{0.5}/R_2, \quad (10)$$

$$\text{At side 1, } k = -V_2(\rho_2 Q/\rho_1)^{0.5}/R_2, \quad (11)$$

$$\sqrt{Q} = \left[ (R_2/R_1 - \sqrt{\rho_1/\rho_2} V_1/V_2) / (R_2/R_1 - R_1/R_2) \right] \pi, \quad (12)$$

$$R_s = R_2 \left[ 1 - (R_2/R_1 - R_1/R_2) / (R_2/R_1 - \sqrt{\rho_1/\rho_2} V_1/V_2) \right]^{0.5}. \quad (13)$$

$R_s$  is the stagnation radius. Since air is the oxidizer in the following study and there is little preferential diffusion effect in the oxidizer side ( $Le_o \approx 1$ ), we will use the stretch rate in the fuel side as the stretch rate for both the opposed jet flame and the opposed tubular flame.

### 4. Results and discussions

For premixed flames, the fuel and oxygen are mixed first, so the flame is curved to the premixture either positively (convex to the premixture) or negatively (concave to the premixture). For diffusion flames, the fuel and oxygen are in different sides of the curved flame surface, so the flame surface is positively curved to one stream and negatively curved to the other one. Since the curvature effects will be related to the preferential diffusion and the oxidizer is air ( $Le_o \approx 1$ ) in the following calculation, the terms of “negatively curved” and “positively curved” refer to the curvature status of the fuel stream here; that is, “negatively curved flame” means that the flame surface is concave to the fuel stream; “positively curved flame” means that the flame surface is convex to the fuel stream.

Except stated otherwise, the following settings are used for  $H_2$  diffusion flames. The fuel is 80%

$N_2$  and 20%  $H_2$ ; the oxidizer is air; the chemistry is from [30]. For the opposed jet burner, the distance between two nozzles is set to 45 mm and the equal velocities are used for the nozzles. For the opposed tubular burner,  $R_1 = 0.3$  mm and  $R_2 = 15$  mm. The stagnation radius for both positively curved flames (fuel from the outer nozzle) and negatively curved flames (fuel from the inner nozzle) are 5 mm. The pressure is atmospheric pressure.

The flame radius can be chosen to be at the peak temperature position or the stoichiometric position that is different from the stagnation position. The distance between the stagnation position and the peak temperature position or the stoichiometric position decreases with stretch rate and is small compared to the stagnation radius for the cases we are studying here. For convenience, we choose the stagnation radius to represent the flame radius approximately.

First, we want to clarify that the diffusion flame parameters are functions of stretch rate and curvature only in the opposed tubular flame; they are independent of the burner geometry. Figure 3 compares the flame temperature variation with stretch rate for different opposed tubular burner geometries and velocity ratios while keeping flame curvature constant (positively curved). For geometry one,  $R_1 = 0.3$  mm;  $R_2 = 15$  mm;  $|V_1/V_2| = 5.538$ . For geometry two,  $R_1 = 1.5$  mm;  $R_2 = 25$  mm;  $|V_1/V_2| = 0.562$ . For geometry three,  $R_1 = 1$  mm;  $R_2 = 20$  mm;  $|V_1/V_2| = 1.138$ . All the three geometry and velocity ratio settings give the same constant curvature, i.e.  $R_s = 5$  mm. From Fig. 3, we can see that the opposed tubular flames have same peak temperature for the same stretch rate and are extinguished at the same stretch rate ( $1590$  s $^{-1}$ ).

Figure 4 shows the comparison of the flame temperature variation with stretch rate for the planar and curved flames. For the opposed jet flame and positively curved flame, the flame temperature decreases monotonically with stretch rate; for the negatively curved flame, the flame temperature first increases and then decreases with

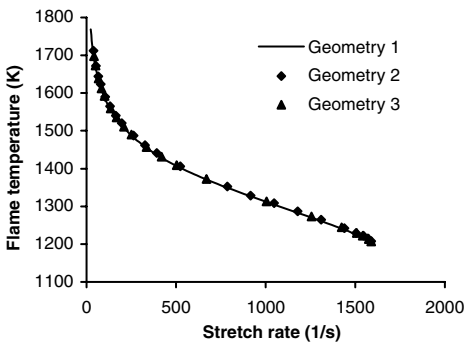


Fig. 3. Flame temperature variation with stretch rate for the positively curved flames with different geometries.

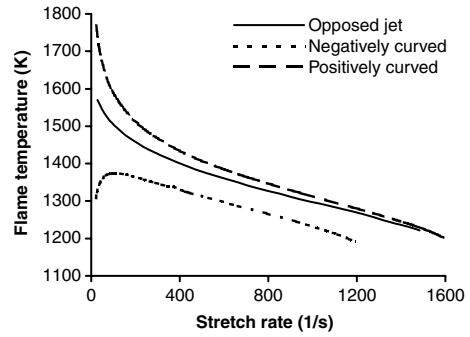


Fig. 4. Flame temperature variation with stretch rate for the planar and curved flames.

stretch rate. The positively curved flame has higher flame temperature and a little bit higher extinction stretch rate ( $1590$  s $^{-1}$ ) than the opposed jet flame ( $1482$  s $^{-1}$ ); the temperature difference decreases with stretch rate. The negatively curved flame has lower flame temperature and extinction stretch rate ( $1192$  s $^{-1}$ ) than the opposed jet flame. As the stretch rate increases, the residence time of the reactants in the reaction zone decreases and the chemical reactions are more incomplete. It is the natural result that the flame temperature of diffusion flames decreases with stretch rate. The fact that the temperature increases with low values of stretch rate for the negatively curved flame is surprising and it must result from the curvature.

The flame temperature of diffusion flames is determined by two factors: the preferential diffusion and the completeness of chemical reactions that is related to Damköhler number. Damköhler number is defined as the ratio of the diffusion time to the chemical reaction time and it reflects the completeness of chemical reactions. For a second order reaction,  $Da = \varpi/(\rho\chi)$  where  $\varpi$  is the chemical reaction rate and  $\chi = \alpha(\partial\xi/\partial x)^2$  is the scalar dissipation rate ( $\alpha$  is the thermal diffusivity;  $\xi$  is the mixture fraction;  $x$  is the axial coordinate for the opposed jet flame and radial coordinate for the opposed tubular flame).

To separate the effect of these two factors, we first set the chemistry to be infinitely fast, so that we can study the preferential diffusion effect independently. Figure 5 shows the flame temperature variation with stretch rate for the three flames with infinite chemistry (one-step irreversible reaction with a very high reaction rate). For the opposed jet flame, the flame temperature is constant ( $1771$  K) but higher than its adiabatic equilibrium value ( $1368.5$  K); this result is consistent with the previous analytical work [3–5], the preferential diffusion increases the flame temperature. For the curved flames, we can see that the positive curvature strengthens the preferential diffusion (higher temperature) and the negative curvature weakens the preferential diffusion (lower

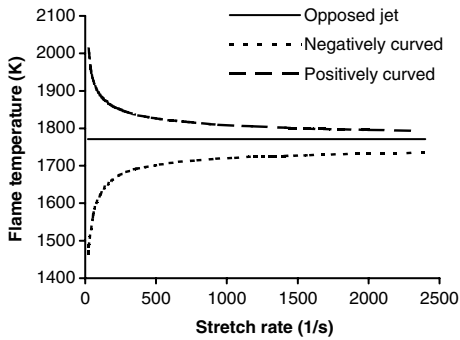


Fig. 5. Flame temperature variation with stretch rate for the planar and curved flames (with infinitely fast chemistry).

temperature). As the stretch rate increases, the flames become thinner and the curvature effect on the preferential diffusion becomes smaller (smaller temperature difference). This means, for diffusion flames, positive curvature strengthens the preferential diffusion and negative curvature weakens the preferential diffusion; the strengthening or weakening effect is proportional to the ratio of flame thickness to flame radius (constant in this example). This result is similar to that of premixed flames [31].

Secondly the completeness of chemical reactions is related to the scalar dissipation rate. Figure 6 shows the variation of  $\chi_{st}$  with stretch rate for the three flames in Fig. 4;  $\xi = (X_{O,2}/W_2v_O + X_F/Wv_F - X_O/Wv_O)/(X_{O,2}/W_2v_O + X_{F,1}/W_1v_F)$  [32];  $v_O$  and  $v_F$  are the stoichiometric coefficients for oxygen and fuel, respectively; the subscripts F, O refer to fuel and oxygen, the second subscripts 1, 2 mean fuel and oxidizer stream boundaries.  $\chi_{st}$  is evaluated at  $\xi = \xi_{st} = 0.624$ . For the same stretch rate, the negatively curved flame has almost the same scalar dissipation rate as the opposed jet flame; and the positively curved flame has higher value than the opposed jet flame, but the difference is small. So the flame tempera-

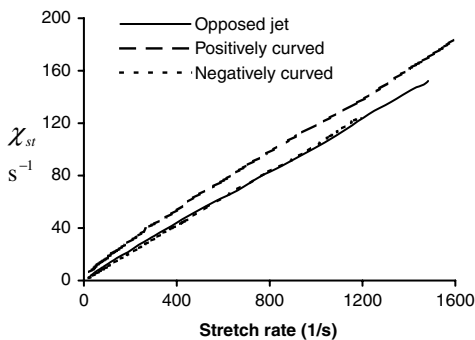


Fig. 6. Scalar dissipation rate variation with stretch rate for the planar and curved flames.

ture difference between the curved flames and the opposed jet flame is mainly caused by the preferential diffusion (by two ways: directly from the preferential diffusion as shown in Fig. 5 and indirectly from Damköhler number through the reaction term).

The above analysis on the preferential diffusion is consistent with all the results of previous work [10–21]. For the perturbed opposed jet flames [16–21], the flames have lower flame temperature and can be extinguished if the  $H_2/N_2$  fuel stream has negative curvature since the negative curvature weakens the preferential diffusion effect; vice versa, the flames have higher flame temperature if the  $H_2/N_2$  fuel stream has positive curvature. It is observed that the preferential diffusion effect increases with decreasing the stretch rate [18]; according our analysis, it results from the flame thickness increasing with decreasing the stretch rate.

To further prove the above analysis on the preferential diffusion, we change the flame thickness while keeping the flame curvature constant, and change the flame curvature while keeping the flame thickness constant. Figure 7 shows the flame temperature variation with the flame radius for the curved flames with constant stretch rate ( $200\text{ s}^{-1}$ ). For constant stretch rate, the flame thickness is almost constant. As the flame radius decreases, the ratio of flame thickness to flame radius increases; the strengthening and weakening effect of the flame curvature on the preferential diffusion becomes stronger; the positively curved flame has higher temperature and the negatively curved flame has lower temperature. Figure 8 shows the flame temperature variations with pressure for constant stretch rate ( $200\text{ s}^{-1}$ ) and constant flame radius. Since Damköhler number is proportional to pressure for the second order reaction ( $\varpi \propto P^2$  and  $\rho\chi \propto P$ , so  $Da \propto P$ ); as the pressure increases, it becomes larger and the chemical reactions are more complete; so the flame temperature increases for all three flames

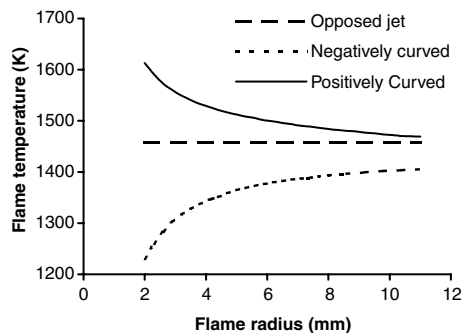


Fig. 7. Flame temperature variation with flame radius for the curved flames with constant stretch rate ( $k = 200\text{ s}^{-1}$ ).

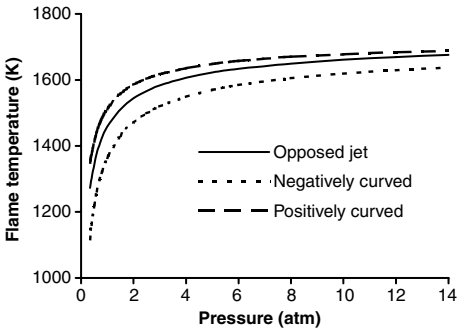


Fig. 8. Flame temperature variation with pressure for the planar and curved flames with constant stretch rate ( $k = 200 \text{ s}^{-1}$ ).

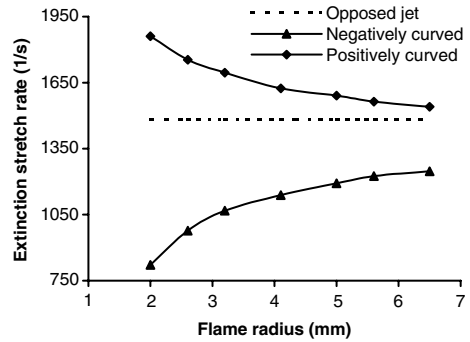


Fig. 10. Extinction stretch rate variation with flame radius for the curved flames.

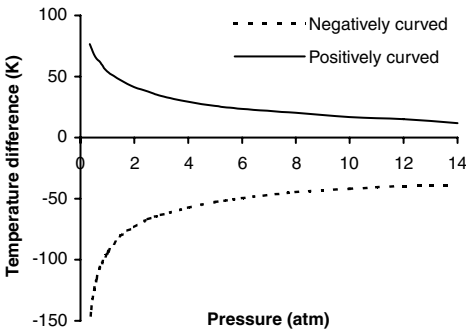


Fig. 9. Flame temperature difference variation with pressure for the curved flames with constant stretch rate ( $k = 200 \text{ s}^{-1}$ ).

[33]. Figure 9 shows the flame temperature difference (minus the flame temperature of the opposed jet flame) variations with pressure. As the pressure increases; the flames become thinner; the ratios of flame thickness to flame radius decrease and the flame temperature differences between the opposed jet flame and the curved flames become smaller.

As we have analyzed the mechanism of the curvature effects on diffusion flames, we now go back to Fig. 4. For the positively curved flame, as the stretch rate increases, both the preferential diffusion and incompleteness of chemical reactions cause the flame temperature to decrease monotonically. For the negatively curved flame, as the stretch rate increases, the preferential diffusion tends to increase the flame temperature while the incompleteness of chemical reactions tends to decrease the flame temperature. At low stretch rate, the ratio of flame thickness to flame radius is large, the preferential diffusion effect dominates and the flame temperature increases with stretch rate; at high stretch rate, the ratio of flame thickness to flame radius is small, the incompleteness of chemical reactions dominates and the flame temperature decreases with stretch rate.

Figure 10 shows the extinction stretch rate variations with curvature. The negatively curved flame extinguishes at lower stretch rate and the positively curved flame extinguishes at higher stretch rate than the opposed jet flame; the extinction stretch rate differences from that of the opposed jet flame decrease with the flame radius. This result is consistent with the flame temperature analysis. Flame curvature plays an important role in extinction if the Lewis numbers are far away from unity and the ratio of flame thickness to flame radius is large, i.e., on the order of unity.

For the  $\text{CH}_4/\text{N}_2$ -air diffusion flames, the temperature difference between the planar and curved flames should be small as shown in Fig. 11 (60%  $\text{CH}_4$ , 40%  $\text{N}_2$ ;  $R_1 = 0.3 \text{ mm}$ ,  $R_2 = 15 \text{ mm}$ ,  $R_s = 5 \text{ mm}$ ; Kee et al. mechanism [34]) since both the Lewis numbers of fuel and oxidizer streams are close to one; a little bit larger temperature difference close to extinction comes from the scalar dissipation rate. All three flames have the same extinction scalar dissipation rate  $\chi_{st} = 19.36 \text{ s}^{-1}$  ( $\xi_{st} = 0.112$ ); the flame curvature has little influence on the extinction scalar dissipation rate or Damköhler number if the Lewis numbers are close to one. For the same stretch rate, the planar flame

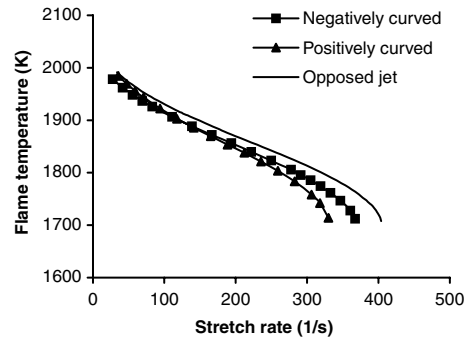


Fig. 11. Flame temperature variation with stretch rate for the planar and curved  $\text{CH}_4/\text{N}_2$  (60%  $\text{CH}_4$ , 40%  $\text{N}_2$ )-air flames.

has lower scalar dissipation rate than the curved flames leading to a higher flame temperature.

Although the above analysis comes from considering the fuel side only, it applies to the oxidizer side too. For negatively (positively) curved fuel stream with Lewis number less than one and positively (negatively) curved oxidizer stream with Lewis number more than one, curvature weakens (strengthens) the flame on both sides. For negatively curved fuel stream with Lewis number less (more) than one and positively curved oxidizer stream with Lewis number less (more) than one, curvature weakens (strengthens) the flame in the fuel side and strengthens (weakens) the flame in the oxidizer side, the comprehensive effect depends on the relative strength between weakening and strengthening.

## 5. Conclusion

A new curved and stretched diffusion flame, i.e., opposed tubular flame that is uniformly stretched and curved, is studied numerically for the first time. The curvature effect is consistent with previous studies. Similar to premixed flames; for diffusion flames, positive curvature strengthens the preferential diffusion and negative curvature weakens the preferential diffusion; the strengthening or weakening effect is proportional the ratio of flame thickness to flame radius. Resulting from the preferential diffusion, curvature has an important influence on extinction if the Lewis numbers are far away from unity and the ratio of flame thickness to flame radius is on the order of unity.

## Acknowledgment

This work is sponsored by National Science Foundation Grant No. CTS-0314704.

## References

- [1] R.J. Kee, F. Rupley, J. Miller, et al., CHEMKIN Collection, Release 3.6, Reaction Design Inc., San Diego, CA, 2000.
- [2] A. Liñan, *Acta Astronautica* 1 (1974) 1007–1039.
- [3] S.H. Chung, C.K. Law, *Combust. Sci. Technol.* 55 (1984) 297–310.
- [4] C.K. Law, S.H. Chung, *Combust. Sci. Technol.* 29 (1982) 129–145.
- [5] B. Cuenot, T. Poinsot, *Combust. Flame* 104 (1996) 111–137.
- [6] I. Glassman, *Combustion*, third ed., Academic Press, San Diego, CA, 1996.
- [7] S.H. Chung, C.K. Law, *Combust. Flame* 52 (1983) 59–79.

- [8] C.J. Sung, J.B. Liu, C.K. Law, *Combust. Flame* 102 (1995) 481–492.
- [9] T.M. Brown, M.A. Tanoff, R.J. Osborne, R.W. Pitz, M.D. Smooke, *Combust. Sci. Technol.* 129 (1997) 71–88.
- [10] S. Ishizuka, *Proc. Combust. Inst.* 19 (1982) 319–326.
- [11] S. Ishizuka, Y. Sakai, *Proc. Combust. Inst.* 21 (1986) 1821–1828.
- [12] H.G. Im, C.K. Law, R.L. Axelbaum, *Proc. Combust. Inst.* 23 (1990) 551–558.
- [13] V.R. Katta, L.P. Goss, W.M. Roquemore, *Combust. Flame* 96 (1994) 60–74.
- [14] T. Takagi, Z. Xu, *Combust. Flame* 96 (1994) 50–59.
- [15] T. Takagi, Z. Xu, M. Komiyama, *Combust. Flame* 106 (1996) 252–260.
- [16] T. Takagi, Y. Yoshikawa, K. Yoshida, M. Komiyama, S. Kinoshita, *Proc. Combust. Inst.* 26 (1996) 1103–1110.
- [17] H. Finke, G. Grünefeld, *Proc. Combust. Inst.* 28 (2000) 2133–2140.
- [18] K. Yoshida, T. Takagi, *JSME Fluid Thermal Eng.* 46 (1) (2003) 190–197.
- [19] J.C. Lee, C.E. Frouzakis, K. Boulouchos, *Combust. Sci. Technol.* 158 (2000) 365–388.
- [20] K. Yoshida, T. Takagi, *Proc. Combust. Inst.* 27 (1998) 685–692.
- [21] V.R. Katta, C.D. Carter, G.J. Fiechtner, W.M. Roquemore, J.R. Gord, J.C. Rolon, *Proc. Combust. Inst.* 27 (1998) 587–594.
- [22] J.A. Wehrmeyer, R.J. Osborne, D.M. Mosbacher, Z. Cheng, R.W. Pitz, C.J. Sung, in: 39th AIAA Aerospace Sciences Meeting and Exhibit, Reno, NV, 8–11 January, 2001, AIAA paper No. 2001-1083.
- [23] P. Wang, J.A. Wehrmeyer, R.W. Pitz, *Combust. Flame* 145 (2006) 401–414.
- [24] G. Dixon-Lewis, V. Giovangigli, R.J. Kee, J.A. Miller, B. Rogg, M.D. Smooke, G. Stahl, J. Warnatz, *Prog. Astro. Aero.* 131 (1991) 125–144.
- [25] M.D. Smooke, V. Giovangigli, *Proc. Combust. Inst.* 23 (1990) 447–454.
- [26] D.M. Mosbacher, J.A. Wehrmeyer, R.W. Pitz, C.J. Sung, J.L. Byrd, *Proc. Combust. Inst.* 29 (2002) 1479–1486.
- [27] R.J. Kee, J.A. Miller, G.H. Evans, G. Dixon-Lewis, *Proc. Combust. Inst.* 22 (1988) 1479–1494.
- [28] S. Hu, P. Wang, R.W. Pitz, M.D. Smooke, *Proc. Combust. Inst.* 31 (2007), 1093–1099.
- [29] K. Seshadri, F.A. Williams, *Intern. J. Heat Mass Transfer* 21 (1978) 251–253.
- [30] M.A. Mueller, T.J. Kim, R.A. Yetter, F.L. Dryer, *Intern. J. Chem. Kinetics* 31 (1999) 113–125.
- [31] P. Wang, R.W. Pitz, AIAA 2004-0148.
- [32] F.A. Williams, *Combustion Theory*, Addison-Wesley, Menlo Park, CA, 1985.
- [33] H.K. Chelliah, C.K. Law, T. Ueda, M.D. Smooke, F.A. Williams, *Proc. Combust. Inst.* 23 (1990) 503–511.
- [34] R.J. Kee, J.F. Grcar, M.D. Smooke, J.A. Miller, Report No. SAND85-8240, Sandia National Laboratories, 1985.

## Comment

*Chih-Jen Sung, Case Western Reserve University, USA.* Since the constant temperature boundary conditions were used in the calculations, did a temperature gradient exist near the cold boundaries for all the low stretch flames studied? If radiation effects were included in your calculations, how would the low stretch flame response be modified for both positively- and negatively-curved flames?

*Reply.* In all the figures, we did not include any result with either temperature or species gradients at the nozzle exits. If there are temperature and species concentration gradients at the boundaries, there will be additional thermal and mass diffusion at the nozzle exits. This extra diffusion will change the flame temperature in a way that is not the result of curvature effects. We paid special attention to this problem and did not show any prediction with temperature and/or species gradients established at the nozzle exits.

If radiation is included in the model, as stretch rate decreases, the flame thickness and radiation increases; thus the flame temperature will decrease and the flame will be extinguished by radiation. With radiation in the model, two extinction limits will be observed. At low stretch rate, the diffusion flame will be extinguished by radiation. At high stretch rate, it will be extinguished by incomplete reaction. Including the radiation effect in the opposed tubular  $H_2/N_2$ -air flame, the flame temperature response to stretch (Fig. 4) will be modified. The positively curved flame temperature will increase with stretch rate at very low stretch rate, peak at some point, and then decrease with stretch rate until the flame is extinguished by incomplete reaction at high stretch rate. For the negatively curved flame, the flame temperature curve will keep its shape; the peak temperature point will move to higher stretch rate and the peak temperature will be lower.